

---

# Annexin V Imaging of Acute Doxorubicin Cardiotoxicity (Apoptosis) in Rats

Roelof J. Bennink, MD<sup>1</sup>; Maurice J. van den Hoff, PhD<sup>2</sup>; Formijn J. van Hemert, PhD<sup>1</sup>; Kora M. de Bruin<sup>1</sup>; Astrid L. Spijkerboer<sup>1</sup>; Jean-Luc Vanderheyden, PhD<sup>3</sup>; Neil Steinmetz, MD<sup>3</sup>; and Berthe L. van Eck-Smit, MD, PhD<sup>1</sup>

<sup>1</sup>Department of Nuclear Medicine, Academic Medical Center, Amsterdam, The Netherlands; <sup>2</sup>Molecular and Experimental Cardiology Group, Department of Anatomy and Embryology, Academic Medical Center, Amsterdam, The Netherlands; and

<sup>3</sup>Theseus Imaging Division, North American Scientific, Boston, Massachusetts

---

Anthracyclines are widely used in chemotherapy regimens for several malignancies, with cardiotoxicity being the major limiting factor in high-dose schedules. Recently, it was reported that doxorubicin induces apoptosis in cardiac muscle cells in vivo and, as such, is expected to be involved in the genesis of doxorubicin-induced cardiomyopathy. The aim of this study was to validate an animal model for in vivo monitoring of doxorubicin cardiotoxicity by means of scintigraphic detection of apoptosis. **Methods:** Three groups of 5 male Wistar rats each were treated for 3, 4, and 5 times with a weekly intraperitoneal injection of doxorubicin at 2.5 mg/kg. At 24 h before and 24 h after the final treatment, <sup>99m</sup>Tc-annexin pinhole scintigraphy was performed. A control group of 5 rats was scanned without doxorubicin treatment. A cardiac uptake ratio was calculated from planar scintigraphy results with the following formula: (mediastinum – fat)/fat. After scintigraphy, the rats were sacrificed, and the heart was processed for histologic analysis. **Results:** Incremental general signs of illness were observed with increasing total cumulative doxorubicin dose. Rats treated for 3, 4, and 5 wk with doxorubicin showed significantly higher uptake ratios of, respectively,  $4.0 \pm 0.52$  (mean  $\pm$  SEM),  $4.8 \pm 0.46$ , and  $5.2 \pm 0.17$  after the final treatment; the ratio for controls was  $1.84 \pm 0.05$  ( $P < 0.05$ ). Histologic analysis confirmed cardiac stress in treated groups, with an increasing left ventricular atrial natriuretic factor messenger RNA expression level with increasing cumulative doxorubicin dose. Late apoptosis was confirmed by terminal deoxynucleotidyltransferase-mediated dUTP nick-end labeling in the rats treated for 5 wk. **Conclusion:** Acute doxorubicin-induced cardiomyopathy based on early apoptosis can be assessed and imaged with annexin V scintigraphy in rats. This finding makes it possible to use this animal model for repetitive noninvasive evaluation of cardioprotective regimens for anthracycline cardiotoxicity.

**Key Words:** apoptosis; cardiotoxicity; annexin V

**J Nucl Med 2004; 45:842–848**

---

Received Sep. 4, 2003; revision accepted Nov. 5, 2003.  
For correspondence or reprints contact: Roelof J. Bennink, MD, Department of Nuclear Medicine, Academic Medical Center, F2-235, Meibergdreef 9, 1105 AZ Amsterdam, The Netherlands.  
E-mail: r.bennink@amc.uva.nl

**D**oxorubicin is a cytotoxic anthracycline that is widely used as a sole chemotherapy or in polychemotherapy regimens for several malignancies. Although the dose-response relationship between anthracycline regimens and remission and event-free survival is well established, cardiotoxicity is the major limiting factor in high-dose schedules (1). Therefore, there is a clinical need for noninvasive investigation of early cardiotoxicity in oncology treatment regimens involving anthracyclines (2).

At present, doxorubicin cardiotoxicity routinely is screened noninvasively by measurement of the left ventricular ejection fraction (3). Despite the fact that ventricular function analysis has continued to prove relevant in defining patient risks, abnormal observations can be made only when cardiac damage already has reached significant proportions. To detect and confirm early anthracycline cardiotoxicity, an endomyocardial biopsy is needed (3). It seemed possible that this invasive test could be replaced by a promising new noninvasive radionuclide in vivo method that uses radioactive monoclonal antibodies (antimyosin) against cardiac muscle (4). The uptake of <sup>111</sup>In-antimyosin by the myocardium occurs only when the integrity of the sarcolemma is lost as a result of cell damage. It has been shown that the intensity of the antibody uptake is related to the cumulative dose of doxorubicin, and its appearance precedes deterioration of the ejection fraction (5). Unfortunately, radionuclide-labeled antimyosin is no longer commercially available. Besides <sup>111</sup>In-antimyosin, <sup>123</sup>I-metaiodobenzylguanidine has been used for the early assessment of doxorubicin cardiotoxicity (6). Unlike the situation with <sup>111</sup>In-antimyosin, which is able to detect myocyte cell damage attributable to doxorubicin cardiotoxicity preceding ejection fraction deterioration, impaired cardiac adrenergic neuron function parallels ejection fraction deterioration and can be detected only with <sup>123</sup>I-metaiodobenzylguanidine studies at higher cumulative doses (6).

Another opportunity for the noninvasive exploration of early cardiomyopathy is to study apoptosis. In the pathophysiology of cardiovascular disease, programmed cell

death of cardiomyocytes has been suggested to be an important contributor because apoptotic cardiomyocytes have been identified during hypoxia, ischemia, cardiac overload, acute myocardial infarction, end-stage heart failure in vivo, and anthracycline use (7,8).

In apoptotic cells, a cascade of events is initiated (9). The early stages of apoptosis include the activation of proteases and sphingomyelinases and the exposure of phospholipid phosphatidylserine on the cell surface. These events occur before the characteristic morphologic changes of plasma membrane bleb formation, vesicle formation, and cytoskeletal disruption, with subsequent cytoplasmic contraction, nuclear chromatin condensation, and DNA fragmentation.

Annexin V is a protein with a high affinity for phosphatidylserine exposed on the cell surface (10). Because under normal circumstances phosphatidylserine is restricted to the inner leaflet of the plasma membrane, annexin V-mediated detection of phosphatidylserine has become an important tool for identifying cells at early stages of apoptosis (10). For the identification of early cardiac stress, monitoring the expression of atrial natriuretic factor (ANF) has been reported (11). Furthermore, ANF has been reported to induce apoptosis in neonatal rat cardiac myocytes (12). At later stages of apoptosis, DNA damage can be observed by an increase in the number of 3' ends prone to labeling with terminal transferase (terminal deoxynucleotidyltransferase-mediated dUTP nick-end labeling [TUNEL] assay) (13).

Recently, noninvasive studies on the diagnosis of acute heart or lung transplant rejection in animals (14) and humans (15) demonstrated that apoptosis occurs during acute cardiac allograft rejection and disappears after the treatment of rejection, indicating the feasibility of the assessment of cardiac apoptosis with  $^{99m}\text{Tc}$ -annexin scintigraphy. Further, it was shown that it is possible to produce acute anthracycline cardiotoxicity involving cardiomyocyte apoptosis with doxorubicin treatment in a rat model (8).

The aims of this study were to correlate doxorubicin-induced apoptosis in rat hearts (visualized by  $^{99m}\text{Tc}$ -annexin scintigraphic imaging) with physiologic features (loss of weight and decreased heart-to-body weight ratio) as well as molecular markers (ANF induction and increased DNA damage) of future heart failure and to validate a tool for the noninvasive assessment of early anthracycline cardiotoxicity.

## MATERIALS AND METHODS

### Study Design

All animal experiments were performed after approval and within the guidelines of the Ethical Animal Research Committee of the University of Amsterdam. Rats were treated with doxorubicin (Pharmacia) to induce acute anthracycline cardiotoxicity involving cardiomyocyte apoptosis as described by Arola et al. (8). Three groups of 5 rats each were treated on a weekly basis for 3, 4, and 5 wk. A control group was treated with saline. At 24 h before and 24 h after the final treatment, rats were injected with  $^{99m}\text{Tc}$ -annexin and examined by pinhole scintigraphy of the thorax.

Immediately after the final scintigraphic examination, the rats were sacrificed, and the heart was removed, cleaned, inspected, weighed, and processed for histologic analysis. The  $^{99m}\text{Tc}$ -annexin uptake ratio was determined and correlated with the heart-to-body weight ratio. In addition, a TUNEL assay (Roche) was performed.

Because of the limited regenerative capacity of cardiomyocytes after birth, cardiomyocyte death attributable to doxorubicin leads to impaired cardiac muscle function. Upon impairment of cardiac function, the adult heart will show compensatory hypertrophy, which may progress to pump failure. In a healthy adult, ventricular ANF messenger RNA (mRNA) is expressed at low levels in the conduction system and is readily induced by hemodynamic changes in the ventricular myocardium (16,17). In pressure overload rat models, changes in sarcoplasmic reticulum  $\text{Ca}^{2+}$ -adenosine triphosphatase 2a (SERCA) mRNA and protein expression levels and calcium processing have been reported (18,19). The prevalent myosin heavy chain (MHC) species in the adult rat ventricle is  $\alpha\text{MHC}$ , which, in the presence of hypertrophy, is downregulated (20). To assess whether doxorubicin-induced cardiomyocyte death also evokes an adaptive response of the remaining myocardium, the patterns of expression of ANF, SERCA, and  $\alpha\text{MHC}$  mRNAs were determined.

### Doxorubicin Cardiotoxicity Model

The rat was chosen as a model for anthracycline-induced cardiomyopathy (21). The rat is an attractive candidate for scintigraphic studies because it is relatively small but its heart, at 1–2 cm, is large enough for scintigraphy (22). Adult male Wistar rats weighing 250 g were purchased from Harlan and maintained under standard conditions at the animal care facility of the Academic Medical Center, Amsterdam, The Netherlands. The rats had free access to standard rodent chow and water. Doxorubicin-induced cardiomyopathy was brought about as described by Arola et al. (8). In brief, after rats received subcutaneous buprenorphine (0.05 mg/kg; Schering-Plough) to provide analgesia, doxorubicin (2.5 mg/kg) was injected intraperitoneally. This treatment was repeated weekly as long as required by the study protocol. Control animals were injected with buprenorphine and saline. The general well-being and the body weight of all animals were monitored weekly.

### Annexin V Labeling

Human annexin V was produced by expression in *Escherichia coli* as described by Tait and Smith (23). The purified protein was derivatized with hydrazinonicotinamide by the method of Abrams et al. (24). To bind  $^{99m}\text{Tc}$  to the hydrazinonicotinamide-annexin V conjugate (kindly provided by North American Scientific, Theseus Imaging Division), 0.8 mL of saline containing approximately 1,000 MBq of pertechnetate was added. Subsequently, 0.02 mL of freshly prepared Sn-Tricine was added to the solution. The reaction vial was incubated for 15 min at room temperature. Radiochemical purity was determined chromatographically with instant thin-layer chromatography paper (Gelman Sciences) as the stationary phase and methyl ethyl ketone as the mobile phase. Labeling efficiency was consistently above 92%, providing a specific activity of 7.4 MBq per microgram of protein. Under these conditions, annexin V labeling was stable for at least 4 h.

### Camera Design

For the imaging of  $^{99m}\text{Tc}$ -annexin uptake in the rat heart, a  $\gamma$ -camera (ARC 3000; Philips) situated in a dedicated animal care facility was equipped with a pinhole collimator fitted with a 3-mm tungsten insert. The pinhole collimator faces up. On top of the

collimator, a specially designed application device is fixed to permit scintigraphy of anterior projections of rats at standardized orientation and distance from the pinhole aperture. The  $\gamma$ -camera is interfaced with a Hermes acquisition and processing station (Nuclear Diagnostics). Static images of the thorax were obtained for 5 min at the 140-keV  $^{99m}\text{Tc}$  peak with a 20% window in a  $128 \times 128$  matrix.

### Scintigraphy and Interpretation

The animals were sedated with ketamine (40 mg/kg)–xylazine (2 mg/kg), given intramuscularly. Once sedated, the rats were injected with 75 MBq of  $^{99m}\text{Tc}$ -annexin (protein concentration, 40  $\mu\text{g}/\text{kg}$ ) intravenously in a tail vein. The animals were scanned 1 h after injection of the radiopharmaceutical in the anterior position but slightly rotated to the left (LAO) to prevent overprojection of bone marrow uptake. Planar anterior pinhole images were displayed on screen, and standardized regions of interest were drawn in the mediastinal cardiac region and in the extrathoracic soft tissue. As a background region, the lung field was avoided because higher annexin V uptake in costal bone marrow after treatment would bias results. A cardiac uptake ratio (CUR) was calculated with the following formula: (mediastinum – fat)/fat. A semiquantitative assessment was preferred over visual interpretation.

### Histologic Examination

After removal, the hearts were fixed for 4 h in ice-cold 4% paraformaldehyde freshly dissolved in phosphate-buffered saline (PBS;  $\text{NaH}_2\text{PO}_4$ – $\text{Na}_2\text{HPO}_4$  at 10 mmol/L and NaCl at 150 mmol/L; pH 7.4) and subsequently transferred to 70% ethanol. After the hearts were cleaved to obtain a 4-chamber view, they were dehydrated in a graded ethanol series and embedded in Paraplast (Tyco). The hearts were sectioned at 7 and 20  $\mu\text{m}$ , and the sections were mounted on aminoalkylsilane-coated slides.

The 7- $\mu\text{m}$  sections were histologically stained with Hematoxylin–Azophloxin (Mochrome) to examine gross anatomy and with Sirius red to assess fibrosis. A TUNEL assay was performed on additional sections according to the instructions of the supplier (13). In short, after deparaffination and rehydration of the sections, endogenous peroxidase activity was blocked by incubation in PBS containing 0.3%  $\text{H}_2\text{O}_2$  and 50% ethanol. Subsequently, nonspecific interactions were blocked by incubation in Tris (10 mmol/L)–EDTA (5 mmol/L)–NaCl (150 mmol/L)–gelatin (0.25%)–Tween 20 (0.05%) (pH 8.0) containing 10% goat serum. Next, the tissue was made accessible by incubation for 10 min with proteinase K (10  $\mu\text{g}/\text{mL}$ ). After labeling of the DNA nicks for 1 h at 37°C with 1 part enzyme solution and 9 parts label solution, which are included in the TUNEL kit, the incorporated fluorescence-labeled dUTP was visualized with a peroxidase-coupled monoclonal antibody directed against fluorescein (1 part converter and 15 parts peroxidase; Roche), diaminobenzidine, and  $\text{H}_2\text{O}_2$  (25). As a negative control, the enzyme was omitted from the assay.

The 20- $\mu\text{m}$  sections were used for nonradioactive in situ hybridization as recently described (26). In short, after deparaffination and rehydration of the sections, the sections were digested with proteinase K (10  $\mu\text{g}/\text{mL}$ ) dissolved in PBS containing 0.05% Tween 20 (PBST) for 15 min. To block proteinase K activity, the sections were washed with 0.2% glycine in PBST for 5 min and then washed twice with PBST for 5 min. The sections were postfixed for 20 min in 4% paraformaldehyde–0.2% glutaraldehyde dissolved in PBS. The sections were prehybridized for at least 1 h at 70°C with hybridization mixture, which consisted of 50% formamide, 5 $\times$  SSC (20 $\times$  SSC is NaCl at 3 mol/L and

trisodium citrate at 0.3 mol/L; pH 4.5), 1% blocking solution (Roche), EDTA (5 mmol/L), 3-[(3-cholamidopropyl)-dimethylammonio]-1-propanesulfonate (0.1%; Sigma), heparin (0.1 mg/mL; BD Biosciences), and yeast total RNA (1 mg/mL; Roche). A digoxigenin-labeled probe then was added to this mixture to a final concentration of 0.5–2  $\mu\text{g}/\text{mL}$ . After hybridization, the sections were rinsed several times and subsequently washed 3 times in 50% formamide, 2 $\times$  SSC, and 0.1% Tween 20 (pH 4.5) for 30 min at 65°C. After 3 washes with PBS–0.1% Tween 20 at room temperature, probe binding to the sections was immunologically detected with a sheep antidigoxigenin Fab fragment covalently coupled to alkaline phosphatase and with nitroblue tetrazolium–5-bromo-4-chloro-3-indolylphosphate as a chromogenic substrate according to the manufacturer's protocol (Roche). After overnight color reaction at room temperature, the reaction was stopped with double-distilled water. Probes specific to rat  $\alpha\text{MHC}$  (27), ANF (28), and SERCA (29) were used.

### Statistical Analysis

Differences among several independent groups were analyzed by the nonparametric Kruskal–Wallis test. Results are expressed as the mean  $\pm$  SEM. All statistical tests were 2-tailed, and differences were evaluated at the 5% level of significance.

## RESULTS

### Scintigraphic Detection of Early Apoptotic Cells

Representative scintigraphic images of a control rat are shown in Figure 1. On scintigraphy, control rats showed faint mediastinal uptake, representing a circulating blood pool. A representative scintigraphic image of a rat treated with doxorubicin is shown in Figure 2. Higher tracer uptake was visible in the cardiac region and in the bone marrow in treated rats than in control rats. Rats treated with doxorubicin for 3, 4, and 5 wk showed a significantly higher ( $P < 0.05$ ) CUR (Table 1). The  $^{99m}\text{Tc}$ -annexin uptake ratio increased after every doxorubicin treatment (Fig. 3) and was

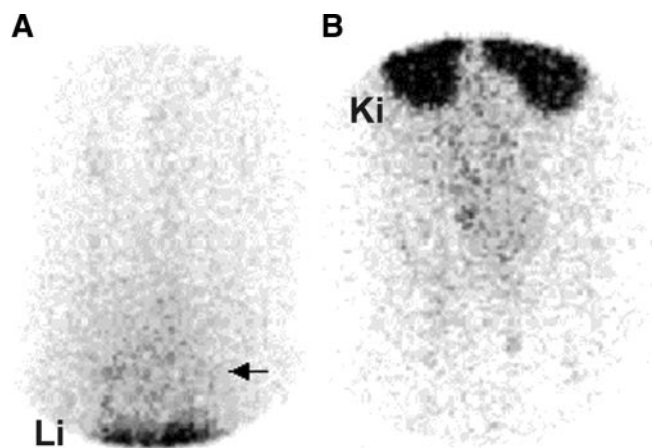


**FIGURE 1.** Planar (LAO) pinhole scintigraphy of a control rat. On images of the thorax including part of the liver (A) and the abdomen (B) at 1 h after intravenous injection of 75 MBq of  $^{99m}\text{Tc}$ -annexin, the physiologic distribution of the radiopharmaceutical, with prominent uptake in the liver (Li) and the kidneys (Ki) and moderate remaining blood-pool activity in the mediastinal region (arrow), is shown.



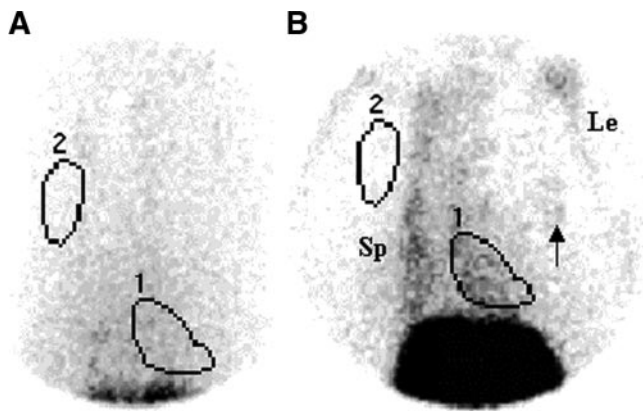


**FIGURE 2.** Planar (LAO) pinhole scintigraphy of the thorax 1 h after intravenous injection of 75 MBq of  $^{99m}\text{Tc}$ -annexin in a control rat (A) and a doxorubicin-treated rat (5 wk; scintigraphy at 24 h after final doxorubicin treatment) (B). Regions of interest were drawn around the cardiac region (1) and in the extrathoracic soft tissue (2) for determination of the CUR. The image in panel B shows pathologic uptake of  $^{99m}\text{Tc}$ -annexin in the cardiac region after treatment with doxorubicin. Note the elevated uptake visible in the bone marrow in the spine (Sp), legs (Le), and ribs (arrow).

higher 1 d after treatment than 1 d before treatment ( $P < 0.05$ ) (Table 1; Fig. 4).

#### Induction of ANF Expression

General histologic staining of heart sections by routine procedures did not show any gross morphologic abnormalities (Hematoxylin-Azophloxin staining) or extensive collagen deposits (Sirius red staining). Interestingly, individual cells with a disorganized cross-striation staining pattern were identified in the trabeculae of the left ventricle in the rats treated with doxorubicin for 5 wk (data not shown).

In situ hybridization analysis of sections showed that ANF mRNA expression was strongly induced in cardiomyocytes flanking the left ventricular lumen (Fig. 5). At this stage, no staining was observed in cardiomyocytes flanking the right ventricular lumen (Fig. 5). On the other hand, the pattern of expression of SERCA, which is expressed in all cardiomyocytes, was not altered.  $\alpha\text{MHC}$  mRNA showed a very low level of expression in the ventricles after 5 wk of treatment (data not shown).

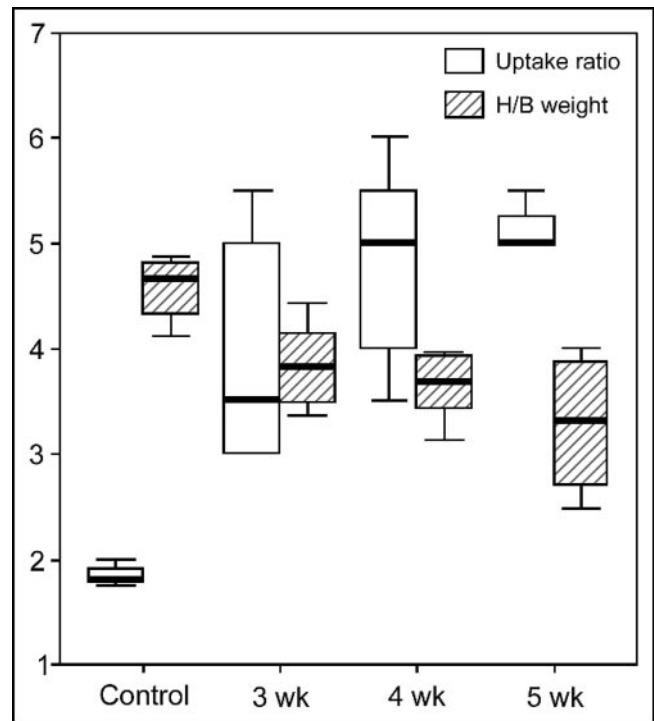


**FIGURE 3.** CUR and heart-to-body-weight ratio in control animals versus rats treated intraperitoneally at 3–5 wk with doxorubicin (mean, interquartile range [box], and outliers). The CUR for  $^{99m}\text{Tc}$ -annexin is significantly higher in treated animals (doxorubicin treatment at 3, 4, and 5 wk) than in control animals ( $P < 0.05$ ). The heart-to-body weight ratio (H/B weight) decreases significantly and progressively with every doxorubicin treatment ( $P < 0.05$ ). The units are reported in thousands.

#### Physiologic Responses to Doxorubicin Treatment

Incremental general signs of illness (growth retardation, general lethargy, and ascites) were observed with increasing total cumulative doxorubicin dose (Table 1). In control rats, the mean  $\pm$  SEM weight gain was  $11.4\% \pm 3.0\%$  per week. In doxorubicin-treated rats, weight gain decreased to a stable level after the first and second treatments, and there was a significant ( $P < 0.001$ ) weight loss of  $2.4\% \pm 1.6\%$  in the last week of treatment. In agreement with increasing signs of illness and weight loss, a decrease in heart weight was observed with increasing total cumulative doxorubicin dose.

**TABLE 1**  
Summary of Groups and Results

Group	No. of treatments	Mean $\pm$ SEM			
		CUR1	CUR2	% Change in body weight	Heart-to-body weight ratio ( $10^3$ )
Control	0	$1.84 \pm 0.05$	NA	$11.41 \pm 3.0$	$4.56 \pm 0.14$
1	3	$2.10 \pm 0.10$	$4.00 \pm 0.52$	$-1.70 \pm 1.2$	$3.85 \pm 0.2$
2	4	$3.10 \pm 0.25$	$4.80 \pm 0.46$	$-2.32 \pm 1.3$	$3.56 \pm 0.19$
3	5	$4.40 \pm 0.30$	$5.17 \pm 0.17$	$-2.40 \pm 1.6$	$3.27 \pm 0.25$

CUR1 = CUR at 24 h before final doxorubicin treatment; CUR2 = CUR at 24 h after final doxorubicin treatment; NA = not applicable.

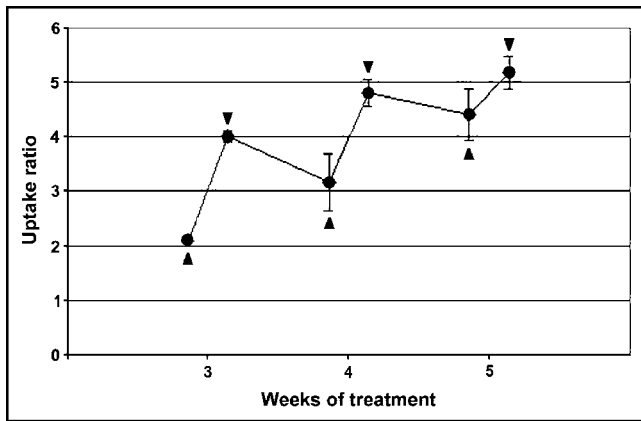


**FIGURE 4.** CUR (mean  $\pm$  SD) at 24 h before ( $\blacktriangle$ ) and 24 h after ( $\blacktriangledown$ ) the final doxorubicin administration to all groups. The saw-like shape and gradual trend upward illustrate the cumulative effect of repetitive doxorubicin administration on apoptosis.

Hearts of treated rats were more dilated than those of control rats. The relative decrease in heart weight was more prominent than the decrease in body weight, as the heart-to-body weight ratio was decreased significantly ( $P < 0.05$ ) at 4 and 5 wk of doxorubicin treatment (Fig. 3). Rats treated 5 times with doxorubicin showed mild abdominal ascites.

#### Detection of Late Apoptotic Cells

To evaluate the role of apoptosis, 2 approaches were taken. Early apoptotic cells were identified scintigraphically by their binding of  $^{99m}\text{Tc}$ -annexin, whereas late apoptotic cells were identified by a TUNEL assay (Fig. 6) (13). Late apoptotic cells were not identified at the early stages of doxorubicin treatment in amounts larger than those in controls. However, significant amounts of late apoptotic cells were identified in the hearts of rats treated for 5 wk. Interestingly, these apoptotic cells were identified only in the myocardial cells flanking the left ventricular lumen. The frequency of apoptotic cells decreased transmurally, and apoptotic cells were absent from the compact left ventricular free wall of the myocardium. Moreover, no apoptotic cells were found in the right ventricular myocardium. A characteristic example is shown in Figure 6. The region of apoptotic cells closely resembles the area of expression of ANF mRNA.

#### DISCUSSION

The type and degree of anthracycline-induced cardiomyopathy, as well as when during or after treatment the condition occurs, are dependent on what risk factors are present (30). Age is a major risk factor. The length of subsequent survival and the amount of somatic growth may influence late anthracycline-associated cardiac outcome. Early cardiotoxicity, occurring during or within 1 y of the completion of treatment, is the greatest risk factor for the development of late cardiomyopathy (30). Anthracyclines induce cardiomyopathy through apoptotic pathways (8). However, it is pos-

sible that, in addition to apoptosis, other known mechanisms contribute to doxorubicin-induced cardiomyopathy; free radical formation and necrosis, which is indicated by the reported elevation of cardiac troponin T in serum (31), may do so. However, histologic analysis showed no cardiomyocyte necrosis in our experiments; therefore, it is possible that annexin V scintigraphy also would have been positive in the presence of necrosis.

The rat model that we used has been shown to produce acute anthracycline cardiotoxicity involving cardiomyocyte apoptosis with doxorubicin treatment (8). The observed apoptosis in this model was dose dependent and cumulative but not additive on repetitive dosing (8). On the basis of these data, we decided to use a weekly doxorubicin dose of 2.5 mg/kg; this dose produced peak cardiomyocyte apoptosis at 24 h after injection and a decrease in apoptosis to nearly the baseline level in the 6 d after this peak.

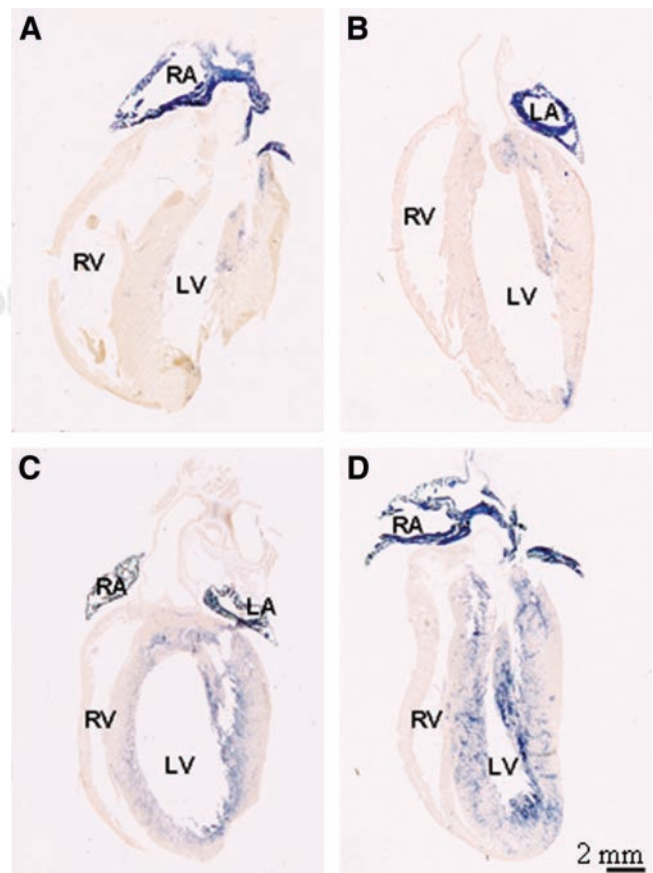


**FIGURE 5.** ANF mRNA expression pattern in hearts of doxorubicin-treated rats. (A) Age-matched control rat after 5 wk of placebo treatment. (B, C, and D) Rats after 3, 4, and 5 wk of doxorubicin treatment, respectively. In control rats (A) and rats treated at 3 wk (B), ANF mRNA is expressed at high levels in the atrial myocardium and in a few scattered cells in the ventricular myocardium. The expression domain expands with ongoing treatment such that virtually all myocardium flanking the left ventricular lumen expresses ANF mRNA after 5 wk of treatment (D). RA = right atrium; LA = left atrium; RV = right ventricle; LV = left ventricle.

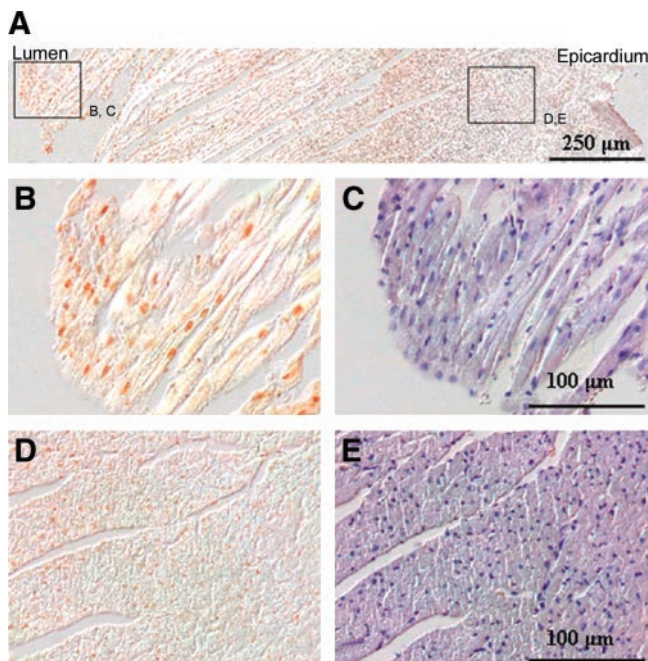


**FIGURE 6.** Late apoptotic cells in the left ventricular free wall of rats treated for 5 wk with doxorubicin. Panels B to E show details of regions indicated in panel A. (B) Detail of the myocardium at the luminal side of the left ventricle in which 30 TUNEL-positive nuclei are present. (C) Section adjacent to that in panel B stained with hematoxylin to identify nuclei. A significantly higher ( $P < 0.01$ ) number of nuclei (156; 19%) is present. (D) Detail of the left ventricular myocardium in which no TUNEL-positive nuclei are present. (E) Presence of 465 nuclei determined by counting of hematoxylin-positive nuclei on a section adjacent to that in panel D. Note the transmural gradient in the frequency of apoptotic nuclei detected by the TUNEL assay, which is highest at the left ventricular luminal side, and the decrease to background levels in the compact (epicardially located) myocardium on the pericardial side of the heart.

The timing of scintigraphy at 60 min after the intravenous injection of  $^{99m}\text{Tc}$ -annexin was based on the described short half-life of annexin V in the circulation without significant redistribution after 30 min, allowing radionuclide imaging within 1 h after injection (32). The baseline mediastinal uptake ratio in control rats most likely is attributable to residual blood activity, which at 1 h after injection is about 3% of the injected dose in mice (10). Delaying imaging to reduce blood-pool activity was not considered because the late-phase plasma clearance is slow (10) and because image count statistics would decrease as a result of radioactive decay. Correcting for blood-pool activity by determining counts in blood and cardiac samples is possible but is not necessary in a semiquantitative organ-specific uptake approach, enabling repetitive measurements.

Our scintigraphic results, obtained by use of  $^{99m}\text{Tc}$ -annexin scintigraphy at 6 d after the injection of doxorubicin, a final weekly injection, and then scintigraphy at 24 h after injection, reproduced (over the various groups) patterns very similar to published observations obtained by histologic analysis of TUNEL-stained images (8). The general

signs of illness observed in this study also matched data reported in the original model (8).

The heart-to-body weight ratio of doxorubicin-treated rats decreased with accumulating dose, suggesting dilated cardiomyopathy. This suggestion also is consistent with immediate postmortem inspection of the heart. As this decrease in cardiac weight might have been the result of cardiomyocyte death, we evaluated whether apoptosis was involved in this process. Apoptosis in the myocardium of healthy rats is a very rare event. To reliably estimate the number of cells undergoing apoptosis in an adult heart, large amounts of cells need to be evaluated. Therefore, small changes in the percentage of apoptotic cells might be missed during analysis of sections of hearts with a TUNEL assay and might underlie the discrepancy observed between the TUNEL assay results and the uptake observed by scintigraphy after 3 and 4 wk of doxorubicin treatment. This annexin V uptake might be the result of other mechanisms that cause cardiac damage in which intracellular phosphatidylserine is exposed, except for fibrosis or necrosis. Interestingly, after 5 wk of doxorubicin treatment, we observed that many of the cardiomyocytes flanking the left ventricular lumen were undergoing apoptosis. The frequency of apoptotic nuclei tapered off quickly transmurally, and no apoptotic nuclei could be detected in the compact layer of the left ventricle. Furthermore, apoptosis was uniquely induced at the left side. In the trabeculae and compact layer of the right ventricle, no apoptotic cells could be identified.

In this study, the specificity of the tracer signal can be questioned. No control protein was used, and as a result of the doxorubicin treatment, the blood-pool activity could have been higher than that in control rats, resulting in an overestimation of myocardial tracer uptake. However, other well-perfused organs, such as the lungs or liver, did not show increased uptake of annexin V as a function of increasing doxorubicin dose (data not shown), supporting the conclusion that overestimation was not imminent.

We observed that ANF mRNA was expressed in the left ventricle of the myocardium at very high levels. ANF influences electrolyte and water balance and modifies peripheral vascular resistance, thereby affecting left ventricular performance. Although the role of ANF in the pathogenesis of congestive heart failure is not clear, it may be useful as an additional, objective early indicator of apoptosis and of hemodynamic compromise in patients susceptible to impaired cardiac function as a result of doxorubicin cardiotoxicity (11,12,33).

It has been reported that some forms of stress can produce transient and reversible phosphatidylserine expression, which may be visualized by  $^{99m}\text{Tc}$ -annexin scintigraphy (34,35). If the stressor remains, it will lead to cell death by apoptosis, whereas cells may be capable of surviving on cessation of the harmful process. In this study, we found that animals receiving a lower cumulative doxorubicin dose showed more early apoptosis (elevated  $^{99m}\text{Tc}$ -annexin CUR) than late apoptosis (TUNEL reaction), supporting this no-



tion. Together, these data suggest that scintigraphy with labeled annexin V may be a very sensitive tool for assessing cardiotoxicity.

$^{99m}\text{Tc}$ -annexin has been used for the visualization of cell death in vivo in patients with acute myocardial infarction (36). Because it has been reported that doxorubicin cardiotoxicity involves cardiomyocyte apoptosis in rats (8) and because the imaging of apoptosis is possible with  $^{99m}\text{Tc}$ -annexin scintigraphy in animals (9) and humans (36), the clinical relevance of the early detection of anthracycline cardiotoxicity (1) is a motivation to pursue further investigation and use our findings in preclinical and clinical settings for oncology patients.

## CONCLUSION

In conclusion, the Wistar rat imaging model with anthracycline-induced cardiomyopathy is based on apoptosis, and  $^{99m}\text{Tc}$ -annexin can be used as a radiopharmaceutical for imaging acute doxorubicin cardiotoxicity. This investigation model may lead to interesting applications in the in vivo evaluation of cardioprotective strategies in preclinical and clinical trials and in monitoring of the cardiotoxicity of existing or novel therapeutic schemes based on anthracycline chemotherapeutics.

## ACKNOWLEDGMENT

This work was financially supported by The Netherlands Heart Foundation (grant M96002).

## REFERENCES

1. Maini CL, Sciuto R, Ferraironi A, et al. Clinical relevance of radionuclide angiography and antimyosin immunoscintigraphy for risk assessment in epirubicin cardiotoxicity. *J Nucl Cardiol.* 1997;4:502–508.
2. Nousiainen T, Jantunen E, Vanninen E, Hartikainen J. Early decline in left ventricular ejection fraction predicts doxorubicin cardiotoxicity in lymphoma patients. *Br J Cancer.* 2002;86:1697–1700.
3. Jain D. Cardiotoxicity of doxorubicin and other anthracycline derivatives. *J Nucl Cardiol.* 2000;7:53–62.
4. Flotats A, Carrio I. Non-invasive in vivo imaging of myocardial apoptosis and necrosis. *Eur J Nucl Med Mol Imaging.* 2003;30:615–630.
5. Valdes OR, Carrio I, Hoefnagel CA, et al. High sensitivity of radiolabelled antimyosin scintigraphy in assessing anthracycline related early myocyte damage preceding cardiac dysfunction. *Nucl Med Commun.* 2002;23:871–877.
6. Carrio I, Estorch M, Berna L, Lopez-Pousa J, Taberero J, Torres G. Indium-111-antimyosin and iodine-123-MIBG studies in early assessment of doxorubicin cardiotoxicity. *J Nucl Med.* 1995;36:2044–2049.
7. Ito H, Shimojo T, Fujisaki H, et al. Thermal preconditioning protects rat cardiac muscle cells from doxorubicin-induced apoptosis. *Life Sci.* 1999;64:755–761.
8. Arola OJ, Saraste A, Pulkki K, Kallajoki M, Parvinen M, Voipio-Pulkki LM. Acute doxorubicin cardiotoxicity involves cardiomyocyte apoptosis. *Cancer Res.* 2000;60:1789–1792.
9. Blankenberg FG, Katsikis PD, Tait JF, et al. Imaging of apoptosis (programmed cell death) with  $^{99m}\text{Tc}$  annexin V. *J Nucl Med.* 1999;40:184–191.
10. Blankenberg FG, Tait JF, Strauss HW. Apoptotic cell death: its implications for imaging in the next millennium. *Eur J Nucl Med.* 2000;27:359–367.
11. Nousiainen T, Vanninen E, Jantunen E, et al. Natriuretic peptides during the

- development of doxorubicin-induced left ventricular diastolic dysfunction. *J Intern Med.* 2002;251:228–234.
12. Wu CF, Bishopric NH, Pratt RE. Atrial natriuretic peptide induces apoptosis in neonatal rat cardiac myocytes. *J Biol Chem.* 1997;272:14860–14866.
13. Gavrieli Y, Sherman Y, Ben-Sasson SA. Identification of programmed cell death in situ via specific labeling of nuclear DNA fragmentation. *J Cell Biol.* 1992;119:493–501.
14. Vriens PW, Blankenberg FG, Stoot JH, et al. The use of technetium Tc 99m annexin V for in vivo imaging of apoptosis during cardiac allograft rejection. *J Thorac Cardiovasc Surg.* 1998;116:844–853.
15. Narula J, Arbustini E, Chandrashekar Y, Schwaiger M. Apoptosis and the systolic dysfunction in congestive heart failure: story of apoptosis interruptus and zombie myocytes. *Cardiol Clin.* 2001;19:113–126.
16. LekanneDeprez RH, van den Hoff MJ, de Boer PA, et al. Changing patterns of gene expression in the pulmonary trunk-banded rat heart. *J Mol Cell Cardiol.* 1998;30:1877–1888.
17. Su X, Brower G, Janicki JS, Chen YF, Oparil S, Dell'Italia LJ. Differential expression of natriuretic peptides and their receptors in volume overload cardiac hypertrophy in the rat. *J Mol Cell Cardiol.* 1999;31:1927–1936.
18. Arai M, Suzuki T, Nagai R. Sarcoplasmic reticulum genes are upregulated in mild cardiac hypertrophy but downregulated in severe cardiac hypertrophy induced by pressure overload. *J Mol Cell Cardiol.* 1996;28:1583–1590.
19. Lompre AM, Anger M, Levitsky D. Sarco(endo)plasmic reticulum calcium pumps in the cardiovascular system: function and gene expression. *J Mol Cell Cardiol.* 1994;26:1109–1121.
20. Schwartz K, Chassagne C, Boheler KR. The molecular biology of heart failure. *J Am Coll Cardiol.* 1993;22:30A–33A.
21. Herman EH, Ferrans VJ. Preclinical animal models of cardiac protection from anthracycline-induced cardiotoxicity. *Semin Oncol.* 1998;25:15–21.
22. Habraken JB, de Bruin K, Shehata M, et al. Evaluation of high-resolution pinhole SPECT using a small rotating animal. *J Nucl Med.* 2001;42:1863–1869.
23. Tait JF, Smith C. Site-specific mutagenesis of annexin V: role of residues from Arg-200 to Lys-207 in phospholipid binding. *Arch Biochem Biophys.* 1991;288:141–144.
24. Abrams MJ, Juweid M, tenKate CI, et al. Technetium-99m-human polyclonal IgG radiolabeled via the hydrazino nicotinamide derivative for imaging focal sites of infection in rats. *J Nucl Med.* 1990;31:2022–2028.
25. Ya J, van den Hoff MJ, de Boer PA, et al. Normal development of the outflow tract in the rat. *Circ Res.* 1998;82:464–472.
26. Moorman AF, Houweling AC, de Boer PA, Christoffels VM. Sensitive non-radioactive detection of mRNA in tissue sections: novel application of the whole-mount in situ hybridization protocol. *J Histochem Cytochem.* 2001;49:1–8.
27. Boheler KR, Chassagne C, Martin X, Wisniewsky C, Schwartz K. Cardiac expressions of alpha- and beta-myosin heavy chains and sarcomeric alpha-actins are regulated through transcriptional mechanisms: results from nuclear run-on assays in isolated rat cardiac nuclei. *J Biol Chem.* 1992;267:12979–12985.
28. Seidman CE, Duly AD, Choi E, et al. The structure of rat preproatrial natriuretic factor as defined by a complementary DNA clone. *Science.* 1984;225:324–326.
29. Lompre AM, de la Bastie D, Boheler KR, Schwartz K. Characterization and expression of the rat heart sarcoplasmic reticulum Ca<sup>2+</sup>-ATPase mRNA. *FEBS Lett.* 1989;249:35–41.
30. Grenier MA, Lipshultz SE. Epidemiology of anthracycline cardiotoxicity in children and adults. *Semin Oncol.* 1998;25:72–85.
31. Auner HW, Tinchon C, Linkesch W, Halwachs-Baumann G, Sill H. Correspondence re: O. J. Arola et al., acute doxorubicin cardiotoxicity involves cardiomyocyte apoptosis. *Cancer Res.*, 60: 1789–1792, 2000. *Cancer Res.* 2001;61:2335–2336.
32. Blankenberg FG, Strauss HW. Non-invasive diagnosis of acute heart- or lung-transplant rejection using radiolabeled annexin V. *Pediatr Radiol.* 1999;29:299–305.
33. Okumura H, Iuchi K, Yoshida T, et al. Brain natriuretic peptide is a predictor of anthracycline-induced cardiotoxicity. *Acta Haematol.* 2000;104:158–163.
34. Strauss HW, Narula J, Blankenberg FG. Radioimaging to identify myocardial cell death and probably injury. *Lancet.* 2000;356:180–181.
35. Narula J, Acio ER, Narula N, et al. Annexin-V imaging for noninvasive detection of cardiac allograft rejection. *Nat Med.* 2001;7:1347–1352.
36. Hofstra L, Liem IH, Dumont EA, et al. Visualisation of cell death in vivo in patients with acute myocardial infarction. *Lancet.* 2000;356:209–212.